Journal of Reproduction and Development, Vol. 64, No 1, 2018

—Original Article—

PAPOLB/TPAP regulates spermiogenesis independently of chromatoid body-associated factors

Shin-ichi KASHIWABARA[1–3)*], Satsuki TSURUTA[1)*], Yutaro YAMAOKA[1)], Kanako OYAMA[1, 2)], Chieko IWAZAKI[1)] and Tadashi BABA[1–3)]

[1)]*Faculty of Life and Environmental Sciences, University of Tsukuba, Ibaraki 305-8572, Japan*
[2)]*PhD Program in Human Biology, School of Integrative and Global Majors, University of Tsukuba, Ibaraki 305-8572, Japan*
[3)]*Life Science Center, Tsukuba Advanced Research Alliance (TARA), University of Tsukuba, Ibaraki 305-8577, Japan*

Abstract. Mutant mice lacking a testis-specific cytoplasmic poly(A) polymerase, PAPOLB/TPAP, exhibit spermiogenesis arrest and male infertility. However, the mechanism by which PAPOLB regulates spermiogenesis remains unclear. In this study, we examined the relationships between PAPOLB and other spermiogenesis regulators present in the chromatoid body (CB). The loss of PAPOLB had no impact either on the abundance of CB components such as PIWIL1, TDRD6, YBX2, and piRNAs, or on retrotransposon expression. In addition, localization of CB proteins and CB architecture were both normal in PAPOLB-null mice. No interactions were observed between PAPOLB and PIWIL1 or YBX2. While PIWIL1 and YBX2 were associated with translationally inactive messenger ribonucleoproteins and translating polyribosomes, PAPOLB was present almost exclusively in the mRNA-free fractions of sucrose gradients. These results suggest that PAPOLB may regulate spermiogenesis through a pathway distinct from that mediated by CB-associated factors.
Key words: Chromatoid body (CB), Spermatogenesis, Testis-specific cytoplasmic poly(A) polymerase β (PAPOLB/TPAP)
(**J. Reprod. Dev. 64:** 25–31, 2018)

Spermatogenesis is a highly specialized process of cellular differentiation comprising several steps; the mitotic proliferation of spermatogonia is followed by two meiotic divisions of spermatocytes that are in turn followed by spermiogenesis, a morphogenetic process that transforms haploid round spermatids into sperm. This differentiation process is orchestrated by a controlled program of stage-specific gene expression, which is regulated at the transcriptional, post-transcriptional, and translational levels [1–6]. We have previously reported that a testis-specific cytoplasmic poly(A) polymerase, PAPOLB/TPAP (poly[A] polymerase β), is responsible for additional poly(A) tail extension of specific mRNAs in round spermatids [7–9]. Loss-of-function mutation in *Papolb* causes impaired spermiogenesis, where the process is arrested at step 7, and results in male infertility [7–9]. Poly(A) tails generally contribute to the stabilization and efficient translation of mRNAs [10, 11], as exemplified by cytoplasmic polyadenylation-induced translational activation of maternal mRNAs with poly(A) tails of ~A_{10} [12, 13]. However, the loss of PAPOLB does not seem to alter the levels of its substrate mRNAs and their translation products [7–9]. Therefore, the mechanism by which PAPOLB regulates spermiogenesis remains enigmatic.

Received: August 6, 2017
Accepted: October 10, 2017
Published online in J-STAGE: November 3, 2017

Correspondence: S Kashiwabara (e-mail: kashiwabara.shin.fw@u.tsukuba.ac.jp)
* S Kashiwabara and S Tsuruta contributed equally to this work.

In many animals, germ cells contain unique cytoplasmic structures called nuage or germinal granules [14]. Chromatoid bodies (CBs) are male germ cell-specific nuage in mammals; CBs have a non-membranous, electron dense perinuclear structure containing micro(mi)RNAs, Piwi-interacting (pi)RNAs, and their associated factors [15–19]. CBs have been thought to be functionally analogous to the somatic processing body (P-body) [20] based on the presence of RNA processing enzymes such as decapping enzyme DCP1a and miRNA pathway components [16]. Although the function(s) of CBs, which include mRNA storage and degradation, are controversial [16, 17, 21], genetic ablation of testis-specific RNA-binding proteins present in CBs, including PIWIL1/MIWI (Piwi-like homolog 1), TDRD6 (Tudor domain-containing 6) that interacts with PIWIL1, and YBX2/MSY2 (Y-box protein 2), arrests spermatogenesis at the round spermatid stage [22–24], highlighting the functional relationship between the CB and spermiogenesis. PIWIL1 belongs to a PIWI-clade of Argonaute proteins, and is implicated in many aspects of RNA metabolism such as post-transcriptional retrotransposon silencing and biogenesis and/or stability of a specific set of miRNAs and piRNAs, as well as stability, translation, and transport of mRNAs [25–30]. YBX2, an RNA-binding protein specific to male and female germ cells, is thought to be involved in mRNA storage and translational repression during gametogenesis [31–33]. Mice lacking PAPOLB exhibit arrested spermiogenesis at developmental stages similar to those exhibited by PIWIL1-, TDRD6-, or YBX2-null mice, suggesting that the functions of PAPOLB and these CB proteins are likely to be interrelated [7, 22–24].

In an attempt to elucidate the molecular mechanisms of spermiogenesis regulated by PAPOLB, we examined its interaction with CB proteins, as well as the involvement of PAPOLB in the synthesis

of CB constituents, CB formation, retrotransposon silencing, and global translation.

Materials and Methods

Antibodies

Antibodies against murine EIF2C2/AGO2 (eukaryotic translation initiation factor 2C2), EIF4E (eukaryotic translation initiation factor 4E), PAIP2A (polyadenylate binding protein-interacting protein 2A), TDRD6, TNRC6A (trinucleotide repeat containing 6A) and YBX2 were raised by immunizing rabbits with recombinant forms of these proteins; the antibodies produced were purified by affinity chromatography. Briefly, 6 × His-tagged murine EIF2C2 (at positions Met^{1}–Leu^{148}), EIF4E (at Met^{1}–Val^{217}), TDRD6 (at Val^{254}–Leu^{753}), and TNRC6A (at Glu^{601}–His^{1025}) were produced in the BL21(DE3) strain of *Escherichia coli*. 6 × His- and thioredoxin (TRX)-tagged murine PAIP2A (at residues Met^{1}–Tyr^{124}) and YBX2 (at Met^{1}–Gln^{94}) were also expressed in the same strain. Purified inclusion bodies containing EIF4E or TDRD6 were solubilized in 8 M urea and serially diluted to 1 M urea. The other four proteins were purified on a Ni-NTA column (Merck Millipore, Billerica, MA, USA). To prepare affinity ligands for antibody purification, EIF2C2 at residues Met^{1}–Met^{48}, EIF4E at Met^{1}–Val^{217}, PAIP2A at Met^{1}–Tyr^{124}, TNRC6A at Glu^{601}–His^{1025}, and YBX2 at Met^{1}–Gln^{94} were expressed as glutathione *S*-transferase (GST)-fused proteins and purified on a glutathione Sepharose 4B column (GE Healthcare, Piscataway, NJ, USA). TDRD6 at positions Val^{254}–Arg^{525} was produced as a maltose-binding protein (MBP)-fused protein and purified on an Amylose resin column (New England Biolabs, Ipswich, MA, USA). The purified proteins carrying 6 × His tags or both 6 × His and TRX tags were emulsified with Freund's complete or incomplete adjuvant (Becton Dickinson, Franklin Lakes, NJ, USA), and injected intradermally into female New Zealand White rabbits (Japan SLC, Hamamatsu, Shizuoka, Japan) [34]. After fractionation by ammonium sulfate (0–40% saturation), each antiserum was affinity-purified on a Sepharose 4B (GE Healthcare) column conjugated with GST- or MBP-fused protein. Antibodies against EIF4G1 (eukaryotic translation initiation factor 4 gamma 1), PABPC1 (polyadenylate-binding protein 1), PAPOLB, and PIWIL1 were prepared as described previously [34, 35]. A rabbit polyclonal antibody against human ribosomal protein L26 (RPL26; IHC-00093) and mouse monoclonal antibody against β-actin (ACTB; 5441) were obtained from Bethyl Laboratories (Montogomery, TX, USA) and Sigma-Aldrich (St. Louis, MO, USA), respectively. A goat polyclonal antibody against human phosphoglycerate kinase 2 (PGK2; sc-133905) and mouse monoclonal antibody against mouse synaptonemal complex protein 3 (SYCP3; sc-74569) were purchased from Santa Cruz Biotechnology (Dallas, TX, USA).

Immunoblot analysis

Purified populations of pachytene spermatocytes, round spermatids (early haploid cells), and elongating/elongated spermatids (late haploid cells) were prepared by unit gravity sedimentation on 2–4% bovine serum albumin gradients as described previously [36]. Each cell population was at least 80% pure, as judged by cell morphology and immunoblot analyses using stage-specific antibodies. Testicular tissues or germ cells were homogenized at 4°C in buffer A, which consisted of 20 mM Tris/HCl, pH 7.5, 0.15 M NaCl, and 0.5% Nonidet P-40, supplemented with 1 mM dithiothreitol, 1 μg/ml leupeptin, 1 μg/ml pepstatin A, and 0.5 mM phenylmethanesulfonyl fluoride (PMSF), using a Teflon-glass homogenizer (750 rpm, 10 strokes). After incubation at 4°C for 4 h, the homogenates were centrifuged at 13,400 × *g* for 10 min at 4°C. Protein extracts from testes (10 μg) or germ cells (2 μg) were subjected to immunoblot analyses according to the methods described previously [9].

Immunoprecipitation

Antibodies (6 μg) were incubated with Protein A agarose beads (20 μl bed volume; Thermo Fischer Scientific, Waltham, MA, USA) in 1 ml of buffer A at 4°C for 1 h. After washing with the same buffer, the antibody-bound beads were mixed with testicular extracts (1 mg/ml in the homogenization buffer) pre-cleared with Sepharose 4B (40 μl bed volume) and rocked at 4°C for 4 h. After centrifugation, the pellet was washed extensively with buffer A, suspended in 50 μl of the same buffer, mixed with 25 μl of 3 × Laemmli buffer, and subjected to immunoblot analysis. In some cases, EasyBlot anti-rabbit IgG (HRP) (GeneTex, Hsinchu, Taiwan) was used as a secondary antibody to reduce the IgG signals.

Reverse transcription-quantitative polymerase chain reaction (RT-qPCR)

Expression levels of retrotransposons were evaluated by RT-qPCR. Total testicular RNA (1 μg) was isolated using an ISOGEN kit (Nippon Gene, Tokyo, Japan), treated with RQ1 RNase-free DNase (Promega, Madison, WI, USA), and reverse-transcribed in the presence of random hexamers using a Superscript III first-strand synthesis system for RT-PCR (Thermo Fischer Scientific). An aliquot of synthesized cDNA was subjected to PCR using the SYBR Premix Ex Taq™ II (Tli RNase H Plus) (TAKARA Bio, Otsu, Shiga, Japan) in a Thermal Cycle Dice™ TP800 (TAKARA Bio). The mRNA levels were normalized to β-actin (*Actb*) mRNA levels. Data are presented as mean ± SEM ($n \geq 3$). Student's *t*-tests were used for statistical analyses; significance was assumed at $P < 0.05$. Primer sequences used for PCRs are: *Actb*, 5'-AGATCAAGATCATTGCTCCTCCT-3' (sense) and 5'-ACGCAGCTCAGTAACAGTCC-3' (antisense); IAP (Intracisternal A-particle element), 5'-AACCAATGCTAATTTCACCTTGGT-3' (sense) and 5'-GCCAATCAGCAGGCGTTAGT-3' (antisense); LINE-1 (Long interspersed element-1), 5'-GGCGAAAGGCAAACGTAAGA-3' (sense) and 5'-GGAGTGCTGCGTTCTGATGA-3' (antisense); SINE B1 (Short interspersed element B1), 5'-TGAGTTCGAGGCCAGCCTGGTCTA-3' (sense) and 5'-ACAGGGTTTCTCTGTGTAGCCCTG-3' (antisense).

Sucrose density gradient analysis

Sucrose gradient analysis was carried out as described previously with minor modifications [34, 36]. Briefly, testicular tissues (~0.1 g) were homogenized at 4°C in 1 ml of HK buffer (20 mM HEPES/KOH, pH 7.4, 0.1 M KCl) containing 5 mM $MgCl_2$, 0.5% Triton X-100, 0.2 mg/ml cycloheximide, 1 μg/ml leupeptin, 1 μg/ml pepstatin, 0.5 mM PMSF, and 40 U/ml RNaseOUT (Thermo Fischer Scientific) and centrifuged at 13,400 × *g* for 10 min at 4°C. The supernatant solution (0.9 ml) was layered onto a 10–45% sucrose gradient (9.5 ml) prepared in HK buffer containing 5 mM $MgCl_2$ and centrifuged in a Beckman Optima LE-80K ultracentrifuge using a Beckman

SW-41 rotor (Beckman Coulter, Fullerton, CA, USA) at 281,000 × *g* at 4°C for 2 h. Fractions (approximately 1 ml each) were manually collected from the top of the gradient and RNA levels in the fractions were measured by a UV spectrophotometer at 260 nm (Nanodrop, Thermo Fischer Scientific). Aliquots of each fraction were analyzed by immunoblotting or by ethidium bromide staining of ribosomal RNAs (rRNAs) purified using an ISOGEN LS kit (Nippon Gene).

Immunohistological analysis

Testicular tissues were fixed overnight at 4°C in 4% paraformaldehyde in phosphate-buffered saline (PBS, pH 7.2) followed by sequential incubation in 10%, 20%, and 30% sucrose in PBS. The specimens were embedded in a Tissue-Tek O.C.T. compound (Sakura Finetek Japan, Tokyo, Japan) and frozen on dry ice. Sections (8 μm) were prepared in a Leica CM3050 cryostat (Leica Microsystems, Wetzlar, Germany), mounted on MAS coated glass slides (Matsunami Glass, Osaka, Japan), and air-dried. The sections were heat-treated with 10 mM citrate buffer (pH 6.0) at 700 W for 1 min in a microwave oven, washed three times with PBS, and permeabilized with 0.1% Triton X-100 in PBS for 20 min. After washing three times with PBS, the slides were blocked with 3% normal goat serum (Vector Laboratories, Burlingame, CA, USA) in PBS containing 0.05% Tween-20, incubated with primary antibodies, and treated with goat anti-rabbit IgG (H+L) conjugated with Alexa Fluor 488 as a secondary antibody (Thermo Fisher Scientific) and 3 μg/ml Alexa Fluor 568-conjugated peanut agglutinin (PNA; Thermo Fischer Scientific). After washing with PBS, the slides were counterstained with 2.5 μg/ml Hoechst 33342 (Thermo Fischer Scientific) in PBS, mounted, and observed under an Olympus IX71 fluorescent microscope (Olympus, Tokyo, Japan).

Transmission electron microscopy (TEM)

Testicular specimens were fixed in 2.5% glutaraldehyde in 0.1 M sodium phosphate (pH 7.4) and then in 0.1 M sodium phosphate (pH 7.4) containing 1% OsO_4. After successive dehydration in a graded series of ethanol and propylene oxide solutions, the specimens were infiltrated with mixtures of propylene oxide and epon (in a ratio of 1:1, followed by a ratio of 1:3) and then in pure epon before being embedded in pure epon. The samples were sliced into 90 nm-thin sections using a Reichert-Jung ultramicrotome (Reichert technologies, Depew, NY, USA), placed on grids, stained with 5% uranyl acetate and lead citrate, and observed using a JEM-1400 transmission electron microscope (JEOL, Tokyo, Japan).

Ethics statement

All animal experiments were approved and performed in compliance with the "Guide for the Care and Use of Laboratory Animals" at the University of Tsukuba (Permit numbers: 14-022, 15-015, 16-008, 17-219).

Results and Discussion

The loss of PAPOLB results in the arrest of spermiogenesis at the round spermatid stage, similar to what is reported in mice lacking PIWIL1, TDRD6, or YBX2 [7, 22–24]. Whether the syntheses of PAPOLB and CB proteins are synchronized during spermatogenesis was the first question to be investigated in this study. The first wave of murine spermatogenesis is initiated shortly after birth, and requires ~35 days to complete; during this process, pachytene spermatocytes, round spermatids, and elongating spermatids begin to appear at postnatal day (p)14, p18, and p28, respectively [37]. Immunoblot analyses showed that these four proteins are present at detectable levels in the testes at p16 (Fig. 1A, left panels), when the most-differentiated cells are in meiotic prophase [37]. Notably, PAPOLB was accumulated gradually during testicular development. In contrast, the levels of the other three proteins increased sharply between p16 and p20 and remained relatively constant afterwards. Next, we analyzed the abundance of these proteins in spermatogenic cell populations purified by unit gravity sedimentation on a BSA gradient [36, 37]. Consistent with developmental accumulation patterns, PAPOLB was most abundantly present in round spermatids, whereas both pachytene spermatocytes and round spermatids contained similar amounts of all CB proteins (Fig. 1A, right panels). Although the accumulation patterns for PAPOLB and the three CB proteins were different, the simultaneous existence of PAPOLB with the three CB proteins in pachytene spermatocytes and round spermatids could indicate that PAPOLB regulates or interacts with these CB proteins. To clarify this, we carried out experiments to investigate if the levels of CB proteins are affected by the absence of PAPOLB. When testicular extracts from the wild-type (*Papolb*$^{+/+}$, +/+), heterozygous (*Papolb*$^{+/-}$, +/–), and homozygous (*Papolb*$^{-/-}$, –/–) mutant mice were analyzed by immunoblotting, extracts from the homozygous mutants contained PIWIL1, TDRD6, and YBX2 at levels comparable to those in the extracts from wild-type and heterozygous littermates (Fig. 1B). Likewise, the levels of two miRNA-associated CB proteins, EIF2C2 and TNRC6A, and piRNAs remained unaffected (Fig. 1B and C).

Since LINE-1 and SINE B1 retrotransposons are de-repressed in some mutant mice lacking CB proteins [18, 28], we then performed RT-qPCR to evaluate the expression levels of LINE-1, IAP, and SINE B1 retrotransposons in the testes at p24, in which round spermatids appear in most seminiferous tubules [22, 37, 38]. Testes at p18, which contain only ~1% round spermatids [37], were also examined. As shown in Fig. 1D, expression of the retrotransposons was still repressed in testes lacking PAPOLB. These results suggest that PAPOLB is not implicated either in the synthesis of CB proteins or in retrotransposon silencing.

As CB proteins are also distributed in the cell cytoplasm [22, 24, 31], where PAPOLB is present [35], we also tested for interactions between PAPOLB and CB proteins using immunoprecipitation and sucrose gradient analyses. Immunoprecipitation analysis of testicular extracts revealed that PAPOLB fails to associate with either PIWIL1 or TDRD6 (Fig. 2A, left panel), although PIWIL1 was complexed with TDRD6 [24, 39]. YBX2 was not included in the complex immunoprecipitated by anti-PAPOLB antibody and *vice versa* (Fig. 2A, right panel). Furthermore, no interaction was observed between YBX2 and PIWIL1. Sucrose gradient analysis of testicular extracts detected PAPOLB in the mRNA-free fractions (fractions 1 and 2, Fig. 2B). In contrast, PIWIL1 and YBX2 were predominantly cosedimented with mRNAs in translationally inactive messenger ribonucleoprotein particles (mRNPs, fractions 3 and 4, Fig. 2B) and in monosomes (fraction 5, Fig. 2B), and with polysomal mRNAs undergoing translation (fractions 6–10, Fig. 2B) [25, 34].

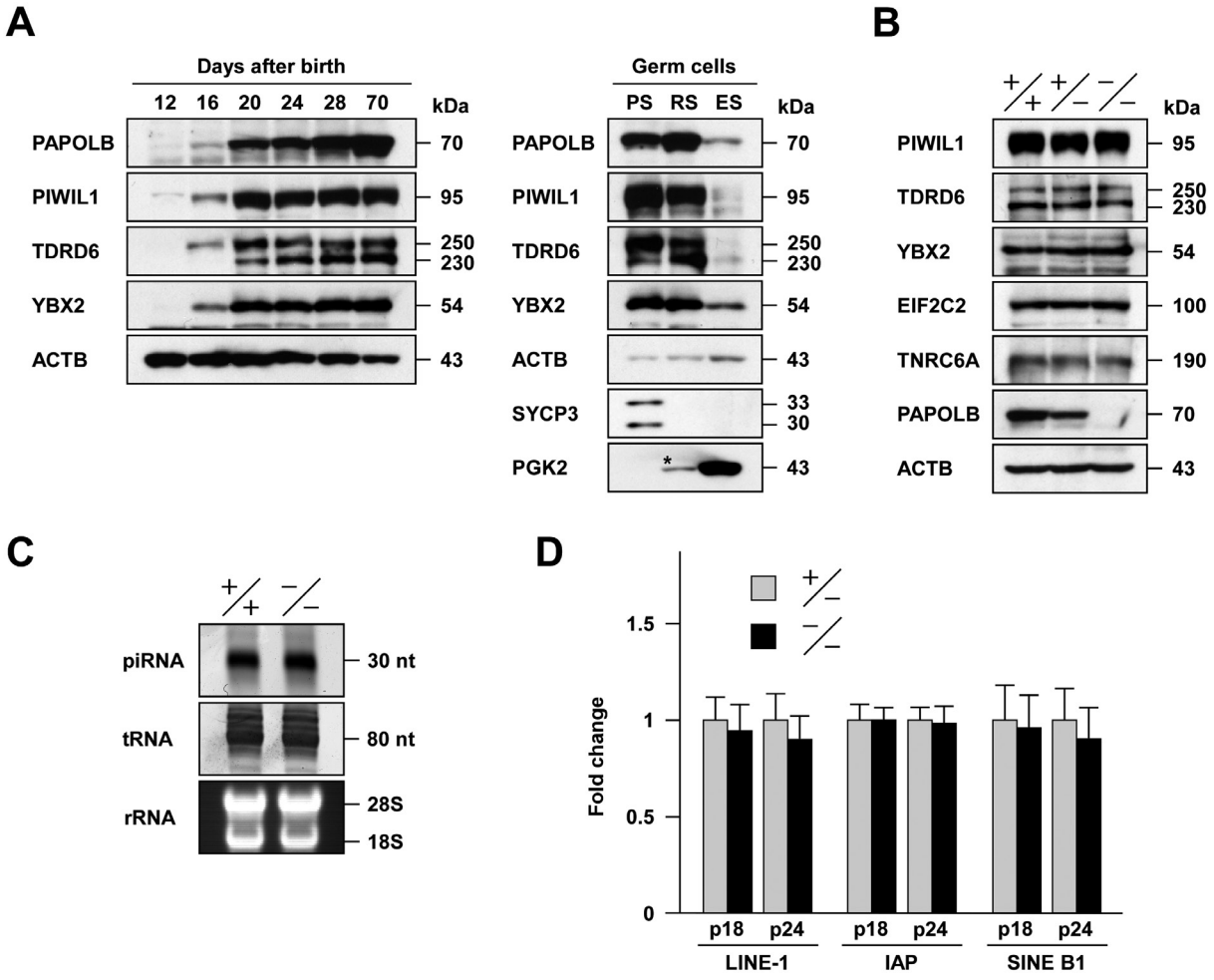

Fig. 1. Quantitative analysis of PAPOLB and CB-associated factors. (A) Accumulation patterns of PAPOLB and CB proteins during spermatogenesis. Protein extracts from juvenile (12–28 days after birth) testes, sexually mature (70 days after birth) testes (10 μg, left panels) and purified populations of spermatogenic cells (2 μg, right panels) were analyzed by immunoblotting using antibodies indicated. ACTB served as a loading control. SYCP3 and PGK2 were used as markers of pachytene spermatocytes and elongating/elongated spermatids, respectively; the PGK2 signal in the round spermatid fraction (asterisk) is derived from contaminating elongating/elongated spermatids. PS, pachytene spermatocytes; RS, round spermatids; ES, elongating/elongated spermatids. (B) Protein levels in PAPOLB-null testes. Testicular protein extracts (10 μg) from the wild-type (+/+), heterozygous (+/–), and homozygous (–/–) mutant mice were subjected to immunoblot analysis using antibodies against the CB proteins indicated. ACTB was used as a loading control. The absence of PAPOLB is clear in the extracts from homozygous mutant testes. (C) piRNA levels in wild-type (+/+) and PAPOLB-null (–/–) mice. Total testicular RNA (10 μg) from the wild-type (+/+) and PAPOLB-null (–/–) mice was separated on a 10% polyacrylamide gel containing 8 M urea and stained with SYBR Gold. The tRNA served as a loading control. The negative image of the gel is shown. The same RNA samples (5 μg) were electrophoresed on agarose gels and stained with ethidium bromide to demonstrate the integrity of the RNA. (D) Retrotransposon expression in the heterozygous (+/–) and homozygous (–/–) mutant testes. Expression levels of LINE-1, IAP, and SINE B1 retrotransposons in heterozygous (+/–) and homozygous (–/–) mutant testes at postnatal day (p)18 and p24 were evaluated by RT-qPCR. Experiments were performed at least three times. Error bars indicate SEM.

Collectively, these results indicate that PAPOLB and the CB proteins are physically separated in the cytoplasm.

In *Tdrd6*$^{-/-}$ mice, some proteins are not correctly localized in CBs and the CBs exhibit less-condensed, dispersed structures [24]. Although PAPOLB had no impact on the synthesis and/or stability of CB proteins (Fig. 1B), it is possible that CB proteins could be mislocalized by the loss of PAPOLB. Immunohistochemical analysis of stage-matched seminiferous tubules (stages II–III and VI–VII) revealed that besides diffuse cytoplasmic staining of pachytene spermatocytes and round spermatids, perinuclear dot-like structures reactive to anti-PIWIL1 or anti-TDRD6 antibody (which correspond to CBs [16, 24, 27]) are present in round spermatids of both the heterozygous and homozygous mutant mice (Fig. 3A). No discernible differences were found in structure, size, and electron density of CBs between the wild-type and PAPOLB-null round spermatids, as analyzed by TEM (Fig. 3B). These observations indicate that the spermiogenic defect in PAPOLB-null mice is not triggered by malformations in CB architecture.

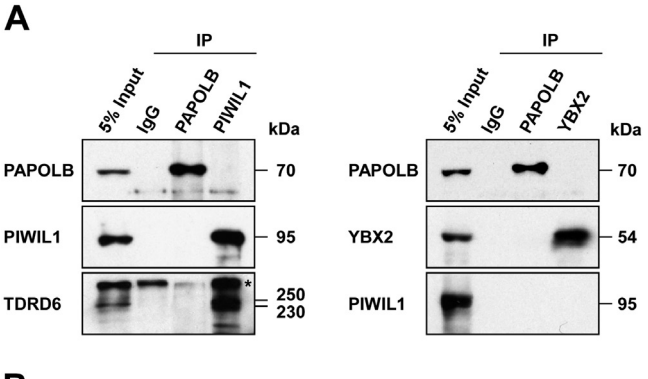

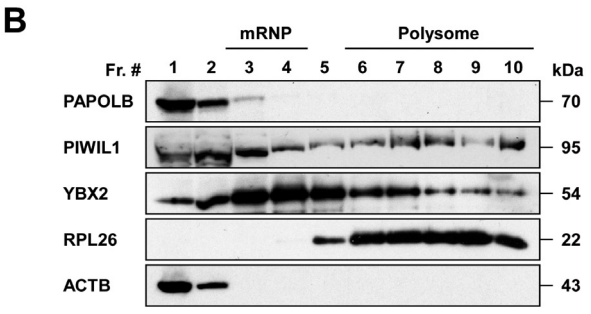

To gain further insight into the molecular mechanism by which PAPOLB regulates spermiogenesis, we examined the effect of PAPOLB deficiency on global translation, using sucrose density gradient ultracentrifugation of p24 testicular extracts. Ethidium bromide staining of total RNAs showed similar distributions of rRNAs between the heterozygous and homozygous mutant testes (Fig. 4A). The ribosomal protein RPL26 was also similarly distributed in both heterozygous and homozygous mutant testes (Fig. 4A). These results suggest that global translation is not hampered by the absence of PAPOLB. Consistent with these results, PAPOLB-null testes at p26

Fig. 2. Immunoprecipitation and sucrose density gradient analyses of CB proteins. (A) Immunoprecipitation analysis of testicular extracts. Testicular extracts (1 mg) were immunoprecipitated (IP) with the antibodies indicated, and analyzed by immunoblotting. One-tenth of the immunoprecipitates were loaded into each lane. Preimmune IgG was used as a negative control. The asterisk represents the position of non-specific signals. (B) Distribution of CB proteins in sucrose gradients. Adult testicular extracts were subjected to 10–45% sucrose gradient ultracentrifugation. Aliquots of each fraction (10 µl) were analyzed by immunoblotting with specific antibodies indicated. ACTB and RPL26 were used to indicate the mRNA-free and polysome fractions, respectively.

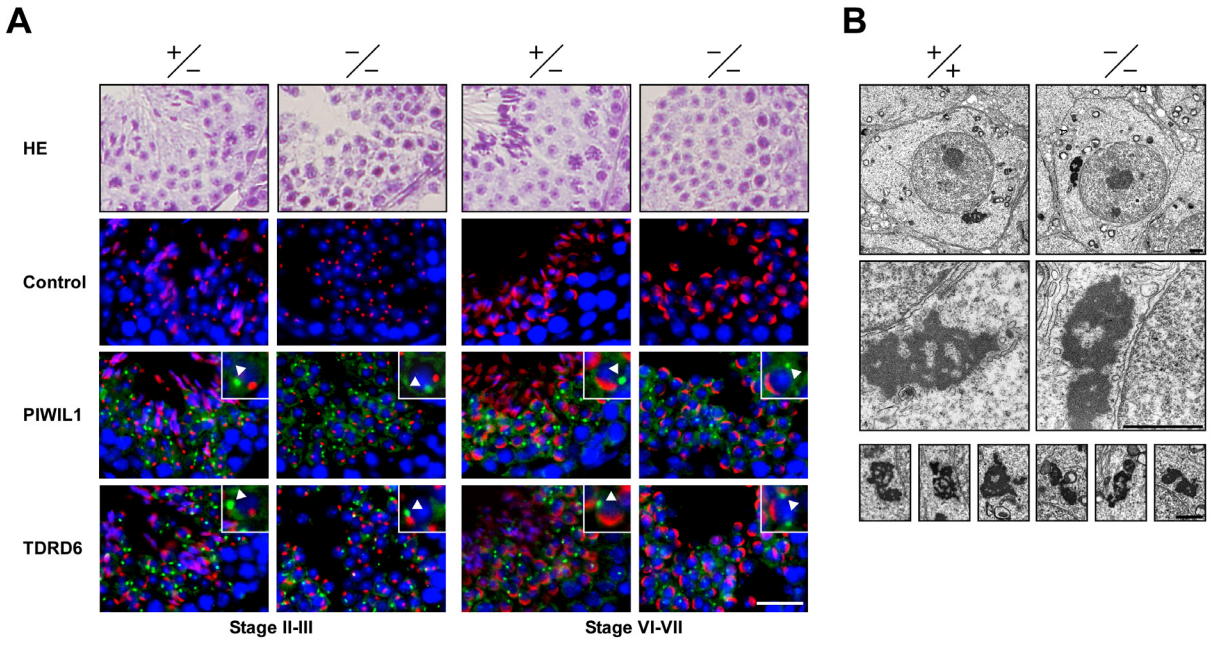

Fig. 3. Histological analysis of CBs. (A) Immunostaining analysis of testicular tissues. Frozen testes sections from the heterozygous (+/–) and homozygous (–/–) mutant mice were incubated with anti-PIWIL1 or anti-TDRD6 antibody followed by Alexa Fluor 488-conjugated secondary antibody (green) and counterstained with Hoechst 33342 (blue). The stages of seminiferous epithelium cycle were identified by acrosome staining with Alexa Fluor 568-conjugated PNA (red). CBs in the enlarged images of round spermatids (insets) are indicated by arrowheads. Preimmune IgG was used as a negative control. Bouin-fixed paraffin sections were stained with hematoxylin and eosin (HE, top panels). Scale bar denotes 50 µm. Note that PAPOLB-deficient testes (–/–) lack elongating and elongated spermatids. (B) Transmission electron microscopy (TEM) of testicular tissues. Ultrathin sections from the wild-type (+/+) and homozygous (–/–) mutant testes were examined by TEM. The middle panels are higher magnification images of the top panels. For further comparison, three different images of CBs from each testis type are also shown at the bottom. Scale bars denote 1 µm. Original magnification is 2,000 × (top and bottom panels), and 12,000 × (middle panels).

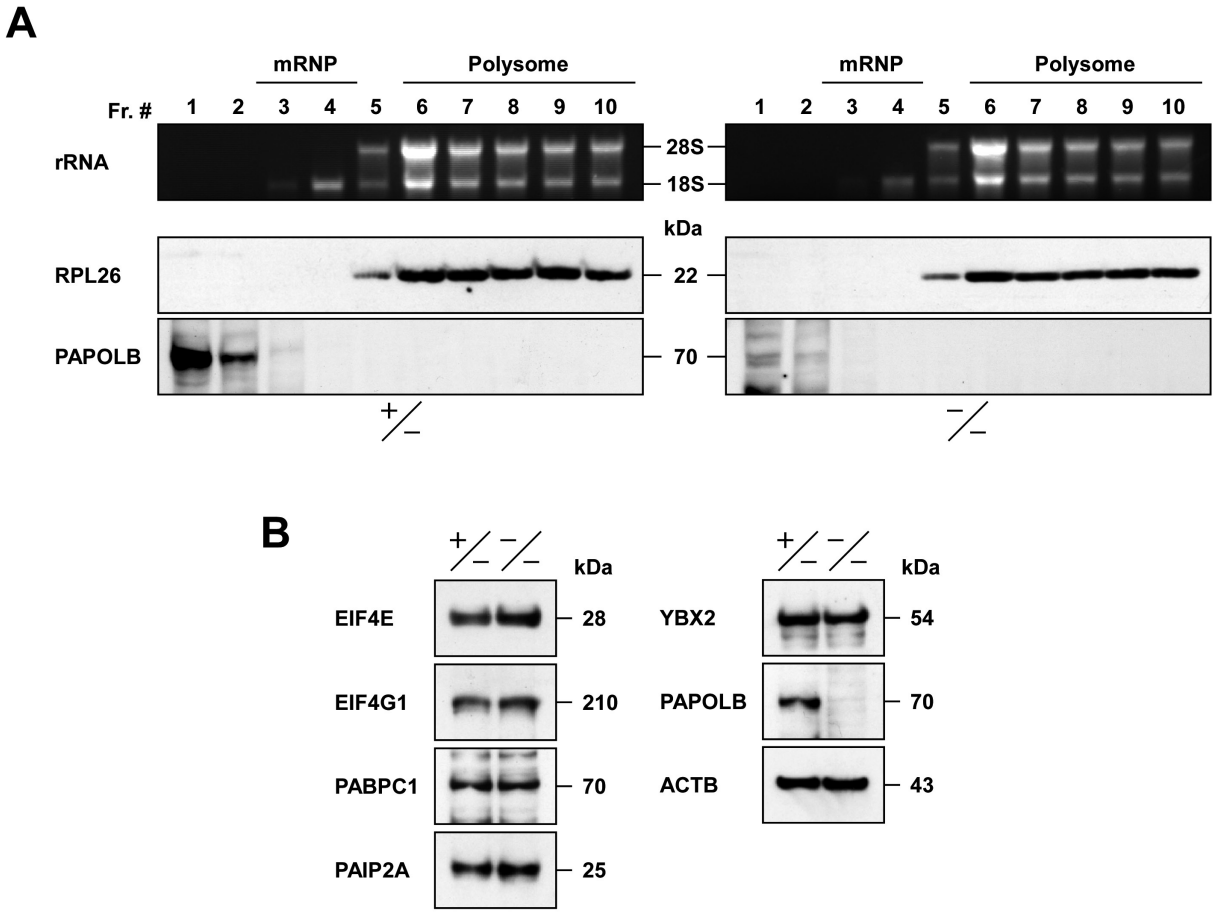

Fig. 4. Global translation. (A) Distribution of polyribosomes in testicular extracts. Testicular extracts from the heterozygous (+/–) and homozygous (–/–) mutant mice at p24 were sedimented in 10–45% sucrose gradients by ultracentrifugation. After fractionation, distributions of rRNAs and RPL26 protein were assessed by ethidium bromide staining and immunoblotting, respectively. PAPOLB is clearly absent in the homozygous (–/–) mutant testes. (B) Protein levels of translation-associated factors. Total testicular extracts (10 μg) from the heterozygous (+/–) and homozygous (–/–) mutant mice at p26 were subjected to immunoblot analysis using the antibodies indicated. ACTB was used as an internal control, and the absence of PAPOLB is clear in the extracts from the null mutants.

contained proteins involved in active translation (EIF4E, EIF4GI, and PABPC1) [40, 41], as well as the translational repressors PAIP2A and YBX2 [32, 42], at levels comparable to those in the testes of heterozygous littermates (Fig. 4B). These observations reinforce the notion that PAPOLB may be involved in the translation of specific mRNAs by cytoplasmic polyadenylation [7–9].

Spermiogenesis requires the two transcription factors, CREMτ (cAMP-responsive element modulator τ) and TBPL1 (TATA-binding protein like-1; also known as TRF2 or TLF). Spermatogenesis in CREM-deficient mice is arrested early during the round spermatid stage (before step 5 of spermiogenesis) and is accompanied by the complete shut-off of haploid-specific gene transcription [43, 44]. Hence, CREMτ is considered to be a master regulator of spermiogenesis. Mice lacking TBPL1 show spermatogenic arrest at a stage later than that observed in CREM-mutant mice (steps 7–14) [38, 45]. Our previous studies indicate that the mRNA and/or protein levels of both transcription factors remain unchanged in PAPOLB-null testes [7–9]. In addition, the translational repressor PAIP2A, the ablation of which results in spermiogenesis arrest at the elongating spermatid stage [46], was normal in p26 testes lacking PAPOLB (Fig. 4B). These observations, taken together with the absence of a detectable relationship between PAPOLB and CB constituents (as shown in this study), imply that spermiogenesis could be governed by multiple independent mechanisms.

Acknowledgements

We thank Ms Junko Sakamoto for her help in performing transmission electron microscopy analysis. This study was supported in part by grants from the Japan Society for the Promotion of Science (grant #22580384) and the Ministry of Education, Sports, Science and Technology (grant #23013005) to SK.

References

1. **Steger K.** Transcriptional and translational regulation of gene expression in haploid spermatids. *Anat Embryol (Berl)* 1999; **199**: 471–487. [Medline] [CrossRef]
2. **Kleene KC.** A possible meiotic function of the peculiar patterns of gene expression in mammalian spermatogenic cells. *Mech Dev* 2001; **106**: 3–23. [Medline] [CrossRef]
3. **Steger K.** Haploid spermatids exhibit translationally repressed mRNAs. *Anat Embryol (Berl)* 2001; **203**: 323–334. [Medline] [CrossRef]
4. **Kimmins S, Kotaja N, Davidson I, Sassone-Corsi P.** Testis-specific transcription mechanisms promoting male germ-cell differentiation. *Reproduction* 2004; **128**: 5–12. [Medline] [CrossRef]
5. **Idler RK, Yan W.** Control of messenger RNA fate by RNA-binding proteins: an emphasis on mammalian spermatogenesis. *J Androl* 2012; **33**: 309–337. [Medline] [CrossRef]
6. **Kleene KC.** Connecting *cis*-elements and *trans*-factors with mechanisms of developmental regulation of mRNA translation in meiotic and haploid mammalian spermatogenic cells. *Reproduction* 2013; **146**: R1–R19. [Medline] [CrossRef]
7. **Kashiwabara S, Noguchi J, Zhuang T, Ohmura K, Honda A, Sugiura S, Miyamoto K, Takahashi S, Inoue K, Ogura A, Baba T.** Regulation of spermatogenesis by testis-specific, cytoplasmic poly(A) polymerase TPAP. *Science* 2002; **298**: 1999–2002. [Medline] [CrossRef]
8. **Zhuang T, Kashiwabara S, Noguchi J, Baba T.** Transgenic expression of testis-specific poly(A) polymerase TPAP in wild-type and TPAP-deficient mice. *J Reprod Dev* 2004; **50**: 207–213. [Medline] [CrossRef]
9. **Kashiwabara SI, Tsuruta S, Okada K, Yamaoka Y, Baba T.** Adenylation by testis-specific cytoplasmic poly(A) polymerase, PAPOLB/TPAP, is essential for spermatogenesis. *J Reprod Dev* 2016; **62**: 607–614. [Medline] [CrossRef]
10. **Sachs A, Wahle E.** Poly(A) tail metabolism and function in eucaryotes. *J Biol Chem* 1993; **268**: 22955–22958. [Medline]
11. **Smith RW, Blee TK, Gray NK.** Poly(A)-binding proteins are required for diverse biological processes in metazoans. *Biochem Soc Trans* 2014; **42**: 1229–1237. [Medline] [CrossRef]
12. **Richter JD.** Cytoplasmic polyadenylation in development and beyond. *Microbiol Mol Biol Rev* 1999; **63**: 446–456. [Medline]
13. **Weill L, Belloc E, Bava F-A, Méndez R.** Translational control by changes in poly(A) tail length: recycling mRNAs. *Nat Struct Mol Biol* 2012; **19**: 577–585. [Medline] [CrossRef]
14. **Eddy EM.** Germ plasm and the differentiation of the germ cell line. *Int Rev Cytol* 1975; **43**: 229–280. [Medline] [CrossRef]
15. **Parvinen M.** The chromatoid body in spermatogenesis. *Int J Androl* 2005; **28**: 189–201. [Medline] [CrossRef]
16. **Kotaja N, Bhattacharyya SN, Jaskiewicz L, Kimmins S, Parvinen M, Filipowicz W, Sassone-Corsi P.** The chromatoid body of male germ cells: similarity with processing bodies and presence of Dicer and microRNA pathway components. *Proc Natl Acad Sci USA* 2006; **103**: 2647–2652. [Medline] [CrossRef]
17. **Kotaja N, Sassone-Corsi P.** The chromatoid body: a germ-cell-specific RNA-processing centre. *Nat Rev Mol Cell Biol* 2007; **8**: 85–90. [Medline] [CrossRef]
18. **Meikar O, Da Ros M, Korhonen H, Kotaja N.** Chromatoid body and small RNAs in male germ cells. *Reproduction* 2011; **142**: 195–209. [Medline] [CrossRef]
19. **Meikar O, Vagin VV, Chalmel F, Sõstar K, Lardenois A, Hammell M, Jin Y, Da Ros M, Wasik KA, Toppari J, Hannon GJ, Kotaja N.** An atlas of chromatoid body components. *RNA* 2014; **20**: 483–495. [Medline] [CrossRef]
20. **Parker R, Sheth U.** P bodies and the control of mRNA translation and degradation. *Mol Cell* 2007; **25**: 635–646. [Medline] [CrossRef]
21. **Kleene KC, Cullinane DL.** Maybe repressed mRNAs are not stored in the chromatoid body in mammalian spermatids. *Reproduction* 2011; **142**: 383–388. [Medline] [CrossRef]
22. **Deng W, Lin H.** *miwi*, a murine homolog of *piwi*, encodes a cytoplasmic protein essential for spermatogenesis. *Dev Cell* 2002; **2**: 819–830. [Medline] [CrossRef]
23. **Yang J, Medvedev S, Yu J, Tang LC, Agno JE, Matzuk MM, Schultz RM, Hecht NB.** Absence of the DNA-/RNA-binding protein MSY2 results in male and female infertility. *Proc Natl Acad Sci USA* 2005; **102**: 5755–5760. [Medline] [CrossRef]
24. **Vasileva A, Tiedau D, Firooznia A, Müller-Reichert T, Jessberger R.** Tdrd6 is required for spermiogenesis, chromatoid body architecture, and regulation of miRNA expression. *Curr Biol* 2009; **19**: 630–639. [Medline] [CrossRef]
25. **Grivna ST, Pyhtila B, Lin H.** MIWI associates with translational machinery and PIWI-interacting RNAs (piRNAs) in regulating spermatogenesis. *Proc Natl Acad Sci USA* 2006; **103**: 13415–13420. [Medline] [CrossRef]
26. **Grivna ST, Beyret E, Wang Z, Lin H.** A novel class of small RNAs in mouse spermatogenic cells. *Genes Dev* 2006; **20**: 1709–1714. [Medline] [CrossRef]
27. **Kotaja N, Lin H, Parvinen M, Sassone-Corsi P.** Interplay of PIWI/Argonaute protein MIWI and kinesin KIF17b in chromatoid bodies of male germ cells. *J Cell Sci* 2006; **119**: 2819–2825. [Medline] [CrossRef]
28. **Reuter M, Berninger P, Chuma S, Shah H, Hosokawa M, Funaya C, Antony C, Sachidanandam R, Pillai RS.** Miwi catalysis is required for piRNA amplification-independent LINE1 transposon silencing. *Nature* 2011; **480**: 264–267. [Medline] [CrossRef]
29. **Nishibu T, Hayashida Y, Tani S, Kurono S, Kojima-Kita K, Ukekawa R, Kurokawa T, Kuramochi-Miyagawa S, Nakano T, Inoue K, Honda S.** Identification of MIWI-associated Poly(A) RNAs by immunoprecipitation with an anti-MIWI monoclonal antibody. *Biosci Trends* 2012; **6**: 248–261. [Medline] [CrossRef]
30. **Goh WSS, Falciatori I, Tam OH, Burgess R, Meikar O, Kotaja N, Hammell M, Hannon GJ.** piRNA-directed cleavage of meiotic transcripts regulates spermatogenesis. *Genes Dev* 2015; **29**: 1032–1044. [Medline] [CrossRef]
31. **Oko R, Korley R, Murray MT, Hecht NB, Hermo L.** Germ cell-specific DNA and RNA binding proteins p48/52 are expressed at specific stages of male germ cell development and are present in the chromatoid body. *Mol Reprod Dev* 1996; **44**: 1–13. [Medline] [CrossRef]
32. **Yu J, Hecht NB, Schultz RM.** RNA-binding properties and translation repression in vitro by germ cell-specific MSY2 protein. *Biol Reprod* 2002; **67**: 1093–1098. [Medline] [CrossRef]
33. **Cullinane DL, Chowdhury TA, Kleene KC.** Mechanisms of translational repression of the *Smcp* mRNA in round spermatids. *Reproduction* 2015; **149**: 43–54. [Medline] [CrossRef]
34. **Kimura M, Ishida K, Kashiwabara S, Baba T.** Characterization of two cytoplasmic poly(A)-binding proteins, PABPC1 and PABPC2, in mouse spermatogenic cells. *Biol Reprod* 2009; **80**: 545–554. [Medline] [CrossRef]
35. **Kashiwabara S, Zhuang T, Yamagata K, Noguchi J, Fukamizu A, Baba T.** Identification of a novel isoform of poly(A) polymerase, TPAP, specifically present in the cytoplasm of spermatogenic cells. *Dev Biol* 2000; **228**: 106–115. [Medline] [CrossRef]
36. **Kashiwabara S, Arai Y, Kodaira K, Baba T.** Acrosin biosynthesis in meiotic and postmeiotic spermatogenic cells. *Biochem Biophys Res Commun* 1990; **173**: 240–245. [Medline] [CrossRef]
37. **Bellvé AR, Cavicchia JC, Millette CF, OBrien DA, Bhatnagar YM, Dym M.** Spermatogenic cells of the prepuberal mouse. Isolation and morphological characterization. *J Cell Biol* 1977; **74**: 68–85. [Medline] [CrossRef]
38. **Zhang D, Penttila T-L, Morris PL, Teichmann M, Roeder RG.** Spermiogenesis deficiency in mice lacking the *Trf2* gene. *Science* 2001; **292**: 1153–1155. [Medline] [CrossRef]
39. **Vagin VV, Wohlschlegel J, Qu J, Jonsson Z, Huang X, Chuma S, Girard A, Sachidanandam R, Hannon GJ, Aravin AA.** Proteomic analysis of murine Piwi proteins reveals a role for arginine methylation in specifying interaction with Tudor family members. *Genes Dev* 2009; **23**: 1749–1762. [Medline] [CrossRef]
40. **Wells SE, Hillner PE, Vale RD, Sachs AB.** Circularization of mRNA by eukaryotic translation initiation factors. *Mol Cell* 1998; **2**: 135–140. [Medline] [CrossRef]
41. **Kahvejian A, Svitkin YV, Sukarieh R, MBoutchou M-N, Sonenberg N.** Mammalian poly(A)-binding protein is a eukaryotic translation initiation factor, which acts via multiple mechanisms. *Genes Dev* 2005; **19**: 104–113. [Medline] [CrossRef]
42. **Khaleghpour K, Svitkin YV, Craig AW, DeMaria CT, Deo RC, Burley SK, Sonenberg N.** Translational repression by a novel partner of human poly(A) binding protein, Paip2. *Mol Cell* 2001; **7**: 205–216. [Medline] [CrossRef]
43. **Nantel F, Monaco L, Foulkes NS, Masquilier D, LeMeur M, Henriksén K, Dierich A, Parvinen M, Sassone-Corsi P.** Spermiogenesis deficiency and germ-cell apoptosis in CREM-mutant mice. *Nature* 1996; **380**: 159–162. [Medline] [CrossRef]
44. **Blendy JA, Kaestner KH, Weinbauer GF, Nieschlag E, Schütz G.** Severe impairment of spermatogenesis in mice lacking the CREM gene. *Nature* 1996; **380**: 162–165. [Medline] [CrossRef]
45. **Martianov I, Fimia G-M, Dierich A, Parvinen M, Sassone-Corsi P, Davidson I.** Late arrest of spermiogenesis and germ cell apoptosis in mice lacking the TBP-like *TLF/TRF2* gene. *Mol Cell* 2001; **7**: 509–515. [Medline] [CrossRef]
46. **Yanagiya A, Delbes G, Svitkin YV, Robaire B, Sonenberg N.** The poly(A)-binding protein partner Paip2a controls translation during late spermiogenesis in mice. *J Clin Invest* 2010; **120**: 3389–3400. [Medline] [CrossRef]